

Charmless hadronic $B_q \rightarrow K_0^*(1430)\overline{K}_0^*(1430)$ decays in the pQCD approach

Xin Liu^{1,2*}, Zhen-Jun Xiao^{2†}, and Zhi-Tian Zou^{3‡}

¹ *Department of Physics and Institute of Theoretical Physics,
Xuzhou Normal University, Xuzhou,
Jiangsu 221116, People's Republic of China*

² *Department of Physics and Institute of Theoretical Physics,
Nanjing Normal University, Nanjing,
Jiangsu 210046, People's Republic of China*

³ *Institute of High Energy Physics, CAS,
P.O.Box 918(4) Beijing 100049, People's Republic of China*

(Dated: May 15, 2021)

Abstract

Based on the assumption of two-quark structure of the scalar $K_0^*(1430)$, the CP-averaged branching ratios(BRs) and CP-violating asymmetries of charmless hadronic $B_q(q = u, d, s, c) \rightarrow K_0^*(1430)\overline{K}_0^*(1430)$ decays are studied in the standard model(SM) by employing the perturbative QCD(pQCD) factorization approach. Our predictions are the following: (1) the CP-averaged BRs for $B_q \rightarrow K_0^*(1430)\overline{K}_0^*(1430)$ decays in both scenarios vary in the range of $10^{-6} \sim 10^{-4}$ in the SM; (2) the magnitudes of $\mathcal{A}_{CP}^{\text{dir}}(B_u \rightarrow K_0^*(1430)^+\overline{K}_0^*(1430)^0)$ and $\mathcal{A}_{CP}^{\text{dir}}(B_{d,s} \rightarrow K_0^*(1430)^+K_0^*(1430)^-)$ in Scenario 1 are much larger than those in Scenario 2 correspondingly; (3) there are no direct CP violations in $B_{d,s} \rightarrow K_0^*(1430)^0\overline{K}_0^*(1430)^0$ and $B_c \rightarrow K_0^*(1430)^+\overline{K}_0^*(1430)^0$ decays in the SM because of the pure penguin and tree topology, respectively. A measurement of our pQCD predictions at the predicted level will favor the $q\bar{q}$ structure of the scalar $K_0^*(1430)$ and help us to understand its physical properties and the involved QCD dynamics.

PACS numbers: 13.25.Hw, 12.38.Bx, 14.40.Nd

* liuxin.physics@gmail.com

† xiaozhenjun@njnu.edu.cn

‡ zouzt@ihep.ac.cn

I. INTRODUCTION

The exclusive non-leptonic weak decays of B_q mesons ($q = (u, d, s, c)$) provide not only good opportunities for testing the Standard Model (SM) but also excellent places for probing different new physics scenarios beyond the SM. Very recently, the Belle collaboration has reported a preliminary upper limit on branching ratio of charmless hadronic $B^0 \rightarrow K_0^*(1430)^0 \bar{K}_0^*(1430)^{01}$ decay [1–3]:

$$Br(B^0 \rightarrow K_0^{*0} \bar{K}_0^{*0}) = 3.21_{-2.85}^{+2.89+2.31} \times 10^{-6} \text{ or } < 8.4 \times 10^{-6} \text{ at 90\% C.L.} \quad (1)$$

where the result is fitted for decay mode with final states $K^+\pi^-K^-\pi^+$ and $Br(K_0^{*0} \rightarrow K^+\pi^-) \approx 66.7\%$. This measurement will be improved soon with the ongoing Large Hadron Collider(LHC) experiments at CERN. At LHC experiments, the b hadrons such as B_u , B_d , B_s , B_c , even Λ_b can be accessed easily. Particularly, the B_c meson could be produced abundantly, which will make a new realm to test the SM, study the heavy flavor dynamics, and explore the involved perturbative and nonperturbative QCD dynamics [4].

In the naive quark model, K_0^* is a p -wave scalar(1^3P_0) particle with quantum number $J^{PC} = 0^{++}$. Lattice calculations [5] on the masses of K_0^* and $a_0(1450)$ indicate a good SU(3) symmetry for the scalar sector, while the latter has been confirmed to be a $\bar{q}q$ meson in lattice calculations [5–9]. Recently, Cheng, Chua, and Yang proposed two possible scenarios based on the assumption of two-quark structure to describe this light scalar K_0^* in the QCD sum rule method [10]: the first excited state in scenario 1(S1) or the lowest lying state in scenario 2(S2), and made extensive studies and interesting analyses phenomenologically on charmless hadronic $B \rightarrow K_0^*(P, V)$ (Here, P and V stand for the light pseudoscalar and vector mesons, respectively) decays to implicate its physical properties in the QCD factorization(QCDF) approach [11, 12]. Moreover, the people also made relevant investigations on K_0^* with other approaches/methods in hadronic B meson decays [13–17].

It is well known that the key point of the theoretical calculation for the charmless hadronic B_q meson decays is how to calculate the hadronic matrix element(HME) reliably. So far, many theoretical approaches/methods, such as naive factorization assumption [18], generalized factorization approach [19], QCDF, soft-collinear effective theory(SCET) [20], and perturbative QCD(pQCD) approach [21–23], are developed to make effective evaluations of HME and interpret the existing rich data. Up to now, the pQCD approach has become one of the most popular methods due to its unique features [24]. The annihilation diagrams, for example, can be evaluated here. While the strong phase for generating CP violation [25] in the pQCD factorization approach, is rather different from that as claimed in SCET [26].

Motivated by the above observations on both experiment and theory aspects, we will investigate the charmless hadronic $B_q \rightarrow K_0^* \bar{K}_0^{*2}$ decays with $q = u, d, s$, and c by employing the low energy effective Hamiltonian [27] and the perturbative QCD(pQCD)

¹ In the following section, we will adopt K_0^* to denote $K_0^*(1430)^+$ and $K_0^*(1430)^0$, and \bar{K}_0^* to stand for $K_0^*(1430)^-$ and $\bar{K}_0^*(1430)^0$ for convenience, respectively, unless otherwise stated.

² Hereafter, for the sake of simplicity, we will adopt B to denote the B_u and B_d mesons, unless otherwise stated.

factorization approach in this work. We here not only calculate the usual factorizable contributions, but also evaluate the nonfactorizable and the annihilation type contributions theoretically. We will predict the physical observables such as CP-averaged branching ratios(BRs) and CP-violating asymmetries in the considered decays. The large BRs and CP violations in the relevant considered decay channels will play an important role in exploring the physical properties of scalar K_0^* . Furthermore, the pure annihilation processes $B_d \rightarrow K_0^{*+} K_0^{*-}$ and $B_c \rightarrow K_0^{*+} \bar{K}_0^{*0}$ could provide interesting information to explore the underlying decay mechanism of the weak annihilation decays.

The paper is organized as follows. In Sec. II, we present the theoretical framework on the low energy effective Hamiltonian and formalism of the pQCD approach. Then we perform the perturbative calculations for the considered $B_q \rightarrow K_0^* \bar{K}_0^*$ decay channels with pQCD approach in Sec. III. The analytic formulas of the decay amplitudes for all the considered modes are also collected in this section. The numerical results and phenomenological analysis are given in Sec. IV. Finally, Sec. V contains the main conclusions and a short summary.

II. THEORETICAL FRAMEWORK

For the considered decays, the related weak effective Hamiltonian H_{eff} [27] can be written as

$$H_{\text{eff}} = \frac{G_F}{\sqrt{2}} \sum_{Q=u,c} V_{Qb}^* V_{QD} \left[C_1(\mu) O_1^{(Q)}(\mu) + C_2(\mu) O_2^{(Q)}(\mu) + \sum_{i=3}^{10} C_i(\mu) O_i(\mu) \right] + \text{H.c.}, \quad (2)$$

with the Fermi constant $G_F = 1.16639 \times 10^{-5} \text{GeV}^{-2}$, Cabibbo-Kobayashi-Maskawa(CKM) matrix elements V , light down type quarks $D = d, s$, and Wilson coefficients $C_i(\mu)$ at the renormalization scale μ . The local four-quark operators $O_i (i = 1, \dots, 10)$ are written as

(1) Current-current(tree) operators

$$O_1^{(Q)} = (\bar{D}_\alpha Q_\beta)_{V-A} (\bar{Q}_\beta b_\alpha)_{V-A}, \quad O_2^{(Q)} = (\bar{D}_\alpha Q_\alpha)_{V-A} (\bar{Q}_\beta b_\beta)_{V-A}; \quad (3)$$

(2) QCD penguin operators

$$\begin{aligned} O_3 &= (\bar{D}_\alpha b_\alpha)_{V-A} \sum_{q'} (\bar{q}'_\beta q'_\beta)_{V-A}, \quad O_4 = (\bar{D}_\alpha b_\beta)_{V-A} \sum_{q'} (\bar{q}'_\beta q'_\alpha)_{V-A}, \\ O_5 &= (\bar{D}_\alpha b_\alpha)_{V-A} \sum_{q'} (\bar{q}'_\beta q'_\beta)_{V+A}, \quad O_6 = (\bar{D}_\alpha b_\beta)_{V-A} \sum_{q'} (\bar{q}'_\beta q'_\alpha)_{V+A}; \end{aligned} \quad (4)$$

(3) Electroweak penguin operators

$$\begin{aligned} O_7 &= \frac{3}{2} (\bar{D}_\alpha b_\alpha)_{V-A} \sum_{q'} e_{q'} (\bar{q}'_\beta q'_\beta)_{V+A}, \quad O_8 = \frac{3}{2} (\bar{D}_\alpha b_\beta)_{V-A} \sum_{q'} e_{q'} (\bar{q}'_\beta q'_\alpha)_{V+A}, \\ O_9 &= \frac{3}{2} (\bar{D}_\alpha b_\alpha)_{V-A} \sum_{q'} e_{q'} (\bar{q}'_\beta q'_\beta)_{V-A}, \quad O_{10} = \frac{3}{2} (\bar{D}_\alpha b_\beta)_{V-A} \sum_{q'} e_{q'} (\bar{q}'_\beta q'_\alpha)_{V-A}. \end{aligned} \quad (5)$$

with the color indices α, β and the notations $(\bar{q}'q')_{V\pm A} = \bar{q}'\gamma_\mu(1 \pm \gamma_5)q'$. The index q' in the summation of the above operators runs through u, d, s, c , and b . The standard combinations a_i of Wilson coefficients are defined as follows,

$$a_1 = C_2 + \frac{C_1}{3}, \quad a_2 = C_1 + \frac{C_2}{3}, \quad a_i = C_i + \frac{C_{i\pm 1}}{3} (i = 3 - 10). \quad (6)$$

where the upper(lower) sign applies, when i is odd(even). Since we work in the leading order $[\mathcal{O}(\alpha_s)]$ of the pQCD approach, it is consistent to use the leading order Wilson coefficients, although the next-to-leading order calculations already exist in the literature [27]. This is the consistent way to cancel the explicit μ dependence in the theoretical formulae. For the renormalization group evolution of the Wilson coefficients from higher scale to lower scale, we use the formulas as given in Ref. [22] directly.

The basic idea of the pQCD approach is that it takes into account the transverse momentum \mathbf{k}_T of the valence quarks in the calculation of the hadronic matrix elements. The B_q meson transition form factors, and the spectator and annihilation contributions are then all calculable in the framework of the \mathbf{k}_T factorization. In the pQCD approach, a $B_q \rightarrow M_2 M_3$ decay amplitude is factorized into the convolution of the six-quark hard kernel(H), the jet function(J) and the Sudakov factor(S) with the bound-state wave functions(Φ) as follows,

$$\mathcal{A}(B_q \rightarrow M_2 M_3) = \Phi_{B_q} \otimes H \otimes J \otimes S \otimes \Phi_{M_2} \otimes \Phi_{M_3}, \quad (7)$$

The jet function J comes from the threshold resummation, which exhibits suppression in the small x (quark momentum fraction) region[28]. The Sudakov factor S comes from the \mathbf{k}_T resummation, which exhibits suppression in the small \mathbf{k}_T region[29, 30]. Therefore, these resummation effects guarantee the removal of the endpoint singularities.

In the practical applications to heavy B_q meson decays, the decay amplitude of Eq. (7) in the pQCD approach can be conceptually written as³,

$$\mathcal{A}(B_q \rightarrow M_2 M_3) \sim \int d^4 k_1 d^4 k_2 d^4 k_3 \text{Tr} [C(t) \Phi_{B_q}(k_1) \Phi_{M_2}(k_2) \Phi_{M_3}(k_3) H(k_1, k_2, k_3, t)], \quad (8)$$

where k_i 's are momenta of light quarks included in each mesons, and Tr denotes the trace over Dirac and color indices. $C(t)$ is the Wilson coefficient which results from the radiative corrections at short distance. In the above convolution, $C(t)$ includes the harder dynamics at larger scale than m_{B_q} scale and describes the evolution of local 4-Fermi operators from m_W (the W boson mass) down to $t \sim \mathcal{O}(\sqrt{\Lambda_{\text{QCD}} m_{B_q}})$ scale, where Λ_{QCD} is the hadronic scale. The function $H(k_1, k_2, k_3, t)$ describes the four quark operator and the spectator quark connected by a hard gluon whose q^2 is in the order of $\Lambda_{\text{QCD}} m_{B_q}$, and includes the $\mathcal{O}(\sqrt{\Lambda_{\text{QCD}} m_{B_q}})$ hard dynamics. Therefore, this hard part H can be perturbatively calculated. The function Φ_M is the wave function which describes hadronization of the quark and anti-quark to the meson M , which is independent of the specific processes and usually determined by employing nonperturbative QCD techniques or other well measured processes.

³ $J(S)$, organizing double logarithms in the hard kernel (meson wave functions), is hidden in H (the three meson states).

Since the b quark is rather heavy, we work in the frame with the B_q meson at rest for simplicity. Throughout this paper, we will use light-cone coordinate (P^+, P^-, \mathbf{P}_T) to describe the meson's momenta with the definitions $P^\pm = \frac{p_0 \pm p_3}{\sqrt{2}}$ and $\mathbf{P}_T = (p_1, p_2)$. For the charmless hadronic $B_u \rightarrow K_0^{*+} \bar{K}_0^{*0}$ decay, for example, assuming that the K_0^{*+} (\bar{K}_0^{*0}) meson moves in the plus (minus) z direction carrying the momentum P_2 (P_3). Then the two final state meson momenta can be written as

$$P_1 = \frac{m_B}{\sqrt{2}}(1, 1, \mathbf{0}_T), \quad P_2 = \frac{m_B}{\sqrt{2}}(1 - r_3^2, r_2^2, \mathbf{0}_T), \quad P_3 = \frac{m_B}{\sqrt{2}}(r_3^2, 1 - r_2^2, \mathbf{0}_T), \quad (9)$$

respectively, where $r_2 = m_{K_0^*}/m_B$ and $r_3 = m_{\bar{K}_0^*}/m_B$. Putting the (light-) quark momenta in B , K_0^* and \bar{K}_0^* mesons as k_1 , k_2 , and k_3 , respectively, we can choose

$$k_1 = (x_1 P_1^+, 0, \mathbf{k}_{1T}), \quad k_2 = (x_2 P_2^+, 0, \mathbf{k}_{2T}), \quad k_3 = (0, x_3 P_3^-, \mathbf{k}_{3T}); \quad (10)$$

Then, for $B_u \rightarrow K_0^{*+} \bar{K}_0^{*0}$ decay, the integration over k_1^- , k_2^- , and k_3^+ will conceptually lead to the decay amplitude in the pQCD approach,

$$\begin{aligned} \mathcal{A}(B_u \rightarrow K_0^{*+} \bar{K}_0^{*0}) &\sim \int dx_1 dx_2 dx_3 b_1 db_1 b_2 db_2 b_3 db_3 \\ &\times \text{Tr} [C(t) \Phi_{B_u}(x_1, b_1) \Phi_{K_0^*}(x_2, b_2) \\ &\times \Phi_{\bar{K}_0^*}(x_3, b_3) H(x_i, b_i, t) S_t(x_i) e^{-S(t)}] . \end{aligned} \quad (11)$$

where b_i is the conjugate space coordinate of \mathbf{k}_{iT} , and t is the largest energy scale in function $H(x_i, b_i, t)$. The large logarithms $\ln(m_W/t)$ are included in the Wilson coefficients $C(t)$. The large double logarithms $(\ln^2 x_i)$ are summed by the threshold resummation [28], and they lead to the jet function $S_t(x_i)$ which smears the end-point singularities on x_i . The last term, $e^{-S(t)}$, is the Sudakov factor which suppresses the soft dynamics effectively [31]. Thus it makes the perturbative calculation of the hard part H applicable at intermediate scale, i.e., m_B scale. We will calculate analytically the function $H(x_i, b_i, t)$ for the considered decays at leading order in α_s expansion and give the convoluted amplitudes in next section.

In the resummation procedures, the heavy B_q meson is treated as a heavy-light system (In the present work, the B_c meson can also be viewed as a heavy-light system although c is the known heavy flavor quark.). In principle there are two Lorentz structures in the B_q meson's wave function. One should consider both of them in calculations. However, since the contribution induced by one Lorentz structure is numerically small [23, 32, 33], and can be neglected approximately, we only consider the contribution from the first Lorentz structure

$$\Phi_{B_q}(k) = \frac{i}{\sqrt{2N_c}} \left[(\not{P} + m_{B_q}) \gamma_5 \phi_{B_q}(k) \right]_{\alpha\beta}, \quad (12)$$

where $P(m)$ is the momentum(mass) of the B_q meson, k is the momentum carried by the light quark in B_q meson, and ϕ_{B_q} is the corresponding distribution amplitude, respectively. In the next section, we will see that the hard part is always independent of one of the

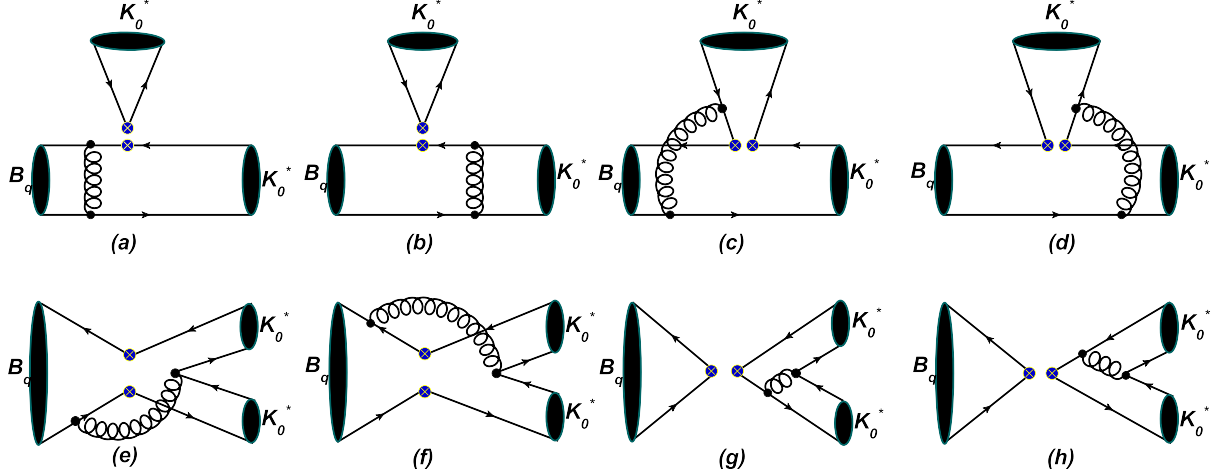


FIG. 1: Typical Feynman diagrams for charmless hadronic $B_q \rightarrow K_0^* K_0^*$ decays at leading order, where $q = u, d, s,$ and $c,$ respectively.

k^+ and/or k^- , if we make the approximations shown in the next section. The B_q meson distribution amplitude $\phi_{B_q}(k)$ is then the function of variables k^- (or k^+) and \mathbf{k}_T only,

$$\phi_{B_q}(k^-, \mathbf{k}_T) = \int \frac{d^4 k}{2\pi} \phi_{B_q}(k^+, k^-, \mathbf{k}_T); \quad (13)$$

The transverse momentum \mathbf{k}_T is usually conveniently converted to the b space parameter by Fourier transformation.

The light-cone wave function of the light scalar K_0^* has been investigated in the QCD sum rule method as [10]

$$\Phi_{K_0^*}(x) = \frac{i}{\sqrt{2N_c}} \left\{ \mathcal{P} \phi_{K_0^*}(x) + m_{K_0^*} \phi_{K_0^*}^S(x) + m_{K_0^*} (\not{n} \not{v} - 1) \phi_{K_0^*}^T(x) \right\}_{\alpha\beta}. \quad (14)$$

where $\phi_{K_0^*}$ and $\phi_{K_0^*}^{S,T}$, and $m_{K_0^*}$ are the leading twist and twist-3 distribution amplitudes, and mass of the scalar K_0^* meson, respectively, while x denotes the momentum fraction carried by quark in the meson, and $n = (1, 0, \mathbf{0}_T)$ and $v = (0, 1, \mathbf{0}_T)$ are the dimensionless light-like unit vectors.

III. PERTURBATIVE CALCULATIONS IN THE PQCD APPROACH

In the following, we will present the analytic factorization formulas for charmless hadronic $B_q \rightarrow K_0^* \bar{K}_0^*$ decays in the pQCD approach. Apart from the factorizable and nonfactorizable spectator diagrams, we can also calculate analytically the annihilation-type ones with no endpoint singularity by employing the pQCD approach. We will adopt F and M to stand for the contributions of factorizable and nonfactorizable diagrams from $(V-A)(V-A)$ operators, F^{P1} and M^{P1} to stand for the contribution from $(V-A)(V+A)$ operators, and F^{P2} and M^{P2} to stand for the contribution from $(S-P)(S+P)$ operators which result from the Fierz transformation of the $(V-A)(V+A)$ operators.

A. $B/B_s \rightarrow K_0^* \bar{K}_0^*$ decays

As illustrated in Fig. 1, when q is u , d or s , all eight types of diagrams may contribute to the $B_{(s)} \rightarrow K_0^* \bar{K}_0^*$ decays. We firstly calculate the usual factorizable spectator(fs) diagrams (a) and (b), in which one can factor out the form factors $B \rightarrow K_0^*$ and $B_s \rightarrow \bar{K}_0^*$. The corresponding Feynman decay amplitudes are given as follows,

(i) $(V - A)(V - A)$ operators:

$$\begin{aligned}
F_{fs} = & -8\pi C_F f_S m_{B_{(s)}}^2 \int_0^1 dx_1 dx_3 \int_0^\infty b_1 db_1 b_3 db_3 \\
& \times \phi_{B_{(s)}}(x_1, b_1) \left\{ [(1+x_3)\phi_S(x_3) + r_S(1-2x_3)(\phi_S^S(x_3) + \phi_S^T(x_3))] \right. \\
& \left. \times h_{fs}(x_1, x_3, b_1, b_3) E_{fs}(t_a) + 2 r_S \phi_S^S(x_3) h_{fs}(x_3, x_1, b_3, b_1) E_{fs}(t_b) \right\} , \quad (15)
\end{aligned}$$

(ii) $(V - A)(V + A)$ operators:

$$F_{fs}^{P1} = F_{fs} , \quad (16)$$

(iii) $(S - P)(S + P)$ operators:

$$\begin{aligned}
F_{fs}^{P2} = & 16\pi C_F \bar{f}_S m_{B_{(s)}}^2 r_S \int_0^1 dx_1 dx_3 \int_0^\infty b_1 db_1 b_3 db_3 \\
& \times \phi_{B_{(s)}}(x_1, b_1) \left\{ [\phi_S(x_3) + r_S[(2+x_3)\phi_S^S(x_3) - x_3\phi_S^T(x_3)]] \right. \\
& \left. \times h_{fs}(x_1, x_3, b_1, b_3) E_{fs}(t_a) + 2 r_S \phi_S^S(x_3) h_{fs}(x_3, x_1, b_3, b_1) E_{fs}(t_b) \right\} ; \quad (17)
\end{aligned}$$

where $r_S = m_S/m_B$ (Hereafter, for simplicity, we will use S to denote K_0^* and its charge conjugation \bar{K}_0^* in the explicit expressions of factorization formulas.) and $C_F = 4/3$ is a color factor. The convolution functions E_i , the factorization hard scales t_i , and the hard functions h_i can be referred to Ref. [34].

For the non-factorizable spectator(nfs) diagrams 1(c) and 1(d), the corresponding decay amplitudes can be written as

(i) $(V - A)(V - A)$ operators:

$$\begin{aligned}
M_{nfs} = & -\frac{32}{\sqrt{6}}\pi C_F m_{B_{(s)}}^2 \int_0^1 dx_1 dx_2 dx_3 \int_0^\infty b_1 db_1 b_2 db_2 \\
& \times \phi_{B_{(s)}}(x_1, b_1) \phi_S(x_2) \left\{ [(1-x_2)\phi_S(x_3) - r_S x_3(\phi_S^S(x_3) - \phi_S^T(x_3))] \right. \\
& \times E_{nfs}(t_c) h_{nfs}^c(x_1, x_2, x_3, b_1, b_2) - h_{nfs}^d(x_1, x_2, x_3, b_1, b_2) \\
& \left. \times [(x_2+x_3)\phi_S(x_3) - r_S x_3(\phi_S^S(x_3) + \phi_S^T(x_3))] E_{nfs}(t_d) \right\} , \quad (18)
\end{aligned}$$

(ii) $(V - A)(V + A)$ operators:

$$\begin{aligned}
M_{nfs}^{P1} = & \frac{32}{\sqrt{6}} \pi C_F m_{B(s)}^2 \int_0^1 dx_1 dx_2 dx_3 \int_0^\infty b_1 db_1 b_2 db_2 \\
& \times \phi_{B(s)}(x_1, b_1) r_S \left\{ [(1 - x_2) \phi_S(x_3) (\phi_S^S(x_2) + \phi_S^T(x_2)) \right. \\
& - r_S (\phi_S^S(x_2) [(x_2 - x_3 - 1) \phi_S^S(x_3) - (x_2 + x_3 - 1) \phi_S^T(x_3)] \\
& + \phi_S^T(x_2) [(x_2 + x_3 - 1) \phi_S^S(x_3) + (1 - x_2 + x_3) \phi_S^T(x_3)])] E_{nfs}(t_c) \\
& \times h_{nfs}^c(x_1, x_2, x_3, b_1, b_2) - h_{nfs}^d(x_1, x_2, x_3, b_1, b_2) E_{nfs}(t_d) \\
& \times [x_2 (\phi_S^S(x_2) - \phi_S^T(x_2)) \phi_S(x_3) + r_S (x_2 (\phi_S^S(x_2) - \phi_S^T(x_2)) \\
& \times (\phi_S^S(x_3) - \phi_S^T(x_3)) + x_3 (\phi_S^S(x_2) + \phi_S^T(x_2)) (\phi_S^S(x_3) + \phi_S^T(x_3)))] \left. \right\} , (19)
\end{aligned}$$

(iii) $(S - P)(S + P)$ operators:

$$\begin{aligned}
M_{nfs}^{P2} = & \frac{32}{\sqrt{6}} \pi C_F m_{B(s)}^2 \int_0^1 dx_1 dx_2 dx_3 \int_0^\infty b_1 db_1 b_2 db_2 \phi_{B(s)}(x_1, b_1) \\
& \times \phi_S(x_2) \left\{ [(x_2 - x_3 - 1) \phi_S(x_3) + r_S x_3 (\phi_S^S(x_3) + \phi_S^T(x_3))] \right. \\
& \times E_{nfs}(t_c) h_{nfs}^c(x_1, x_2, x_3, b_1, b_2) + h_{nfs}^d(x_1, x_2, x_3, b_1, b_2) \\
& \times [x_2 \phi_S(x_3) - r_S x_3 (\phi_S^S(x_3) - \phi_S^T(x_3))] \left. E_{nfs}(t_d) \right\} ; (20)
\end{aligned}$$

In the above three formulas, i.e., Eqs. (18)-(20), one can find that there exist cancelations between the contributions of the two diagrams in Fig. 1(c) and 1(d).

The Feynman diagrams shown in Fig. 1(e) and 1(f) are the non-factorizable annihilation(nfa) ones, whose contributions are

(i) $(V - A)(V - A)$ operators:

$$\begin{aligned}
M_{nfa} = & -\frac{32}{\sqrt{6}} \pi C_F m_{B(s)}^2 \int_0^1 dx_1 dx_2 dx_3 \int_0^\infty b_1 db_1 b_2 db_2 \\
& \times \phi_{B(s)}(x_1, b_1) \left\{ [(1 - x_3) \phi_S(x_2) \phi_S(x_3) - r_S r_S (\phi_S^S(x_2) \right. \\
& \times [(1 + x_2 - x_3) \phi_S^S(x_3) - (1 - x_2 - x_3) \phi_S^T(x_3)] + \phi_S^T(x_2) \\
& \times [(1 - x_2 - x_3) \phi_S^S(x_3) - (1 + x_2 - x_3) \phi_S^T(x_3)])] E_{nfa}(t_e) \\
& \times h_{nfa}^e(x_1, x_2, x_3, b_1, b_2) - E_{nfa}(t_f) h_{nfa}^f(x_1, x_2, x_3, b_1, b_2) \\
& \times [x_2 \phi_S(x_2) \phi_S(x_3) + r_S r_S (\phi_S^S(x_2) [(x_3 - x_2 - 3) \phi_S^S(x_3) \\
& - (1 - x_2 - x_3) \phi_S^T(x_3)] + \phi_S^T(x_2) [(1 - x_2 - x_3) \phi_S^S(x_3) \\
& - (1 - x_2 + x_3) \phi_S^T(x_3)])] \left. \right\} , (21)
\end{aligned}$$

(ii) $(V - A)(V + A)$ operators:

$$\begin{aligned}
M_{nfa}^{P1} = & \frac{32}{\sqrt{6}} \pi C_F m_{B(s)}^2 \int_0^1 dx_1 dx_2 dx_3 \int_0^\infty b_1 db_1 b_2 db_2 \\
& \times \phi_{B(s)}(x_1, b_1) \left\{ [r_S x_2 \phi_S(x_3) (\phi_S^S(x_2) + \phi_S^T(x_2)) + r_S(1 - x_3) \right. \\
& \times \phi_S(x_2) (\phi_S^S(x_3) - \phi_S^T(x_3))] E_{nfa}(t_e) h_{nfa}^e(x_1, x_2, x_3, b_1, b_2) \\
& + [r_S(2 - x_2) (\phi_S^S(x_2) + \phi_S^T(x_2)) \phi_S(x_3) + r_S(1 + x_3) \\
& \left. \times \phi_S(x_2) (\phi_S^S(x_3) - \phi_S^T(x_3))] E_{nfa}(t_f) h_{nfa}^f(x_1, x_2, x_3, b_1, b_2) \right\} , \quad (22)
\end{aligned}$$

(iii) $(S - P)(S + P)$ operators:

$$\begin{aligned}
M_{nfa}^{P2} = & \frac{32}{\sqrt{6}} \pi C_F m_{B(s)}^2 \int_0^1 dx_1 dx_2 dx_3 \int_0^\infty b_1 db_1 b_2 db_2 \\
& \times \phi_{B(s)}(x_1, b_1) \left\{ [(1 - x_3) \phi_S(x_2) \phi_S(x_3) - r_S r_S (\phi_S^S(x_2) \right. \\
& \times [(x_2 - x_3 + 3) \phi_S^S(x_3) - (1 - x_2 - x_3) \phi_S^T(x_3)] + \phi_S^T(x_2) \\
& \times [(1 - x_2 - x_3) \phi_S^S(x_3) + (1 - x_2 + x_3) \phi_S^T(x_3)])] E_{nfa}(t_f) \\
& \times h_{nfa}^f(x_1, x_2, x_3, b_1, b_2) - E_{nfa}(t_e) h_{nfa}^e(x_1, x_2, x_3, b_1, b_2) \\
& \times [x_2 \phi_S(x_2) \phi_S(x_3) + r_S r_S (\phi_S^S(x_2) [(x_3 - x_2 - 1) \phi_S^S(x_3) \\
& - (1 - x_2 - x_3) \phi_S^T(x_3)] + \phi_S^T(x_2) [(1 - x_2 - x_3) \phi_S^S(x_3) \\
& \left. + (1 + x_2 - x_3) \phi_S^T(x_3)])] \right\} ; \quad (23)
\end{aligned}$$

For the last two diagrams in Fig. 1, i.e., the factorizable annihilation(*fa*) diagrams 1(g) and 1(h), we have

(i) $(V - A)(V - A)$ operators:

$$\begin{aligned}
F_{fa} = & -8\pi C_F m_{B(s)}^2 \int_0^1 dx_2 dx_3 \int_0^\infty b_2 db_2 b_3 db_3 \left\{ [x_2 \phi_S(x_2) \phi_S(x_3) - 2r_S r_S \right. \\
& \times ((x_2 + 1) \phi_S^S(x_2) + (x_2 - 1) \phi_S^T(x_2)) \phi_S^S(x_3)] h_{fa}(x_2, 1 - x_3, b_2, b_3) \\
& \times E_{fa}(t_g) - [(1 - x_3) \phi_S(x_2) \phi_S(x_3) + 2r_S r_S \phi_S^S(x_2) ((x_3 - 2) \phi_S^S(x_3) \\
& \left. - x_3 \phi_S^T(x_3))] E_{fa}(t_h) h_{fa}(1 - x_3, x_2, b_3, b_2) \right\} , \quad (24)
\end{aligned}$$

(ii) $(V - A)(V + A)$ operators:

$$F_{fa}^{P1} = F_{fa} , \quad (25)$$

(iii) $(S - P)(S + P)$ operators:

$$\begin{aligned}
F_{fa}^{P2} = & -16\pi C_F m_{B(s)}^2 \int_0^1 dx_2 dx_3 \int_0^\infty b_2 db_2 b_3 db_3 \left\{ [2r_S \phi_S(x_2) \phi_S^S(x_3) \right. \\
& - r_S x_2 (\phi_S^S(x_2) - \phi_S^T(x_2)) \phi_S(x_3)] h_{fa}(x_2, 1 - x_3, b_2, b_3) E_{fa}(t_g) \\
& + [r_S(1 - x_3) \phi_S(x_2) (\phi_S^S(x_3) + \phi_S^T(x_3)) - 2r_S \phi_S^S(x_2) \phi_S(x_3)] \\
& \left. \times E_{fa}(t_h) h_{fa}(1 - x_3, x_2, b_3, b_2) \right\} . \quad (26)
\end{aligned}$$

It is interesting to notice that there is a large cancelation in the factorizable annihilation F_{fa} , i.e., Eq. (24), from the diagrams 1(g) and 1(h), which can result in the tiny or small deviations from zero and can be seen numerically as displayed in the last column of the 2nd line of Tables I and II. In the SU(3) limit, in particular, this cancelation will lead to the exact zero contribution.

B. $B_c \rightarrow K_0^{*+} \bar{K}_0^{*0}$ decay

In the SM, charmless hadronic $B_c \rightarrow K_0^{*+} \bar{K}_0^{*0}$ decay can only occur through the pure annihilation-type diagrams. From the effective Hamiltonian (2), there are 4 types of diagrams contributing to the $B_c \rightarrow K_0^{*+} \bar{K}_0^{*0}$ decay as illustrated in Fig. 1(e)-(h), which result in the Feynman decay amplitudes F'_{fa} and M'_{nfa} from singly current-current operators, respectively. Following the same procedure as stated in the above subsection, we can obtain the analytic decay amplitudes for $B_c \rightarrow K_0^{*+} \bar{K}_0^{*0}$ mode,

$$\begin{aligned}
F'_{fa} &= -8\pi C_F m_{B_c}^2 \int_0^1 dx_2 dx_3 \int_0^\infty b_2 db_2 b_3 db_3 \\
&\times \{ h_{fa}(1-x_3, x_2, b_3, b_2) E'_{fa}(t'_g) [x_2 \phi_S(x_2) \phi_S(x_3) - 2r_S r_S \phi_S^S(x_3) \\
&\times ((x_2+1)\phi_S^S(x_2) + (x_2-1)\phi_S^T(x_2))] - h_{fa}(x_2, 1-x_3, b_2, b_3) E'_{fa}(t'_h) \\
&\times [(1-x_3)\phi_S(x_2)\phi_S(x_3) + 2r_S r_S \phi_S^S(x_2) ((x_3-2)\phi_S^S(x_3) - x_3\phi_S^T(x_3))] \} , (27) \\
M'_{nfa} &= -\frac{16\sqrt{6}}{3} \pi C_F m_{B_c}^2 \int_0^1 dx_2 dx_3 \int_0^\infty b_1 db_1 b_2 db_2 \\
&\times \{ h'_{nfa}(x_2, x_3, b_1, b_2) E'_{nfa}(t'_e) [(r_c - x_3 + 1)\phi_S(x_2)\phi_S(x_3) - r_S r_S (\phi_S^S(x_2) \\
&\times ((3r_c + x_2 - x_3 + 1)\phi_S^S(x_3) - (r_c - x_2 - x_3 + 1)\phi_S^T(x_3)) + \phi_S^T(x_2) \\
&\times ((r_c - x_2 - x_3 + 1)\phi_S^S(x_3) + (r_c - x_2 + x_3 - 1)\phi_S^T(x_3))] - E'_{nfa}(t'_f) \\
&\times [(r_b + r_c + x_2 - 1)\phi_S(x_2)\phi_S(x_3) - r_S r_S (\phi_S^S(x_2)((4r_b + r_c + x_2 - x_3 \\
&- 1)\phi_S^S(x_3) - (r_c + x_2 + x_3 - 1)\phi_S^T(x_3)) + \phi_S^T(x_2)((r_c + x_2 + x_3 - 1) \\
&\times \phi_S^S(x_3) - (r_c + x_2 - x_3 - 1)\phi_S^T(x_3))] h'^f_{nfa}(x_2, x_3, b_1, b_2) \} , (28)
\end{aligned}$$

where the non-relativistic approximation form of the distribution amplitude ϕ_{B_c} for B_c meson has been used, the convolution factor E'_i , the hard scale t'_i , and the hard function h'_i are referred to Refs. [17, 35]. Moreover, $r_b = m_b/m_{B_c}$, $r_c = m_c/m_{B_c}$, and $r_b + r_c \approx 1$ in B_c meson.

C. Decay Amplitudes for $B_q \rightarrow K_0^* \bar{K}_0^*$ ($q = u, d, s, c$) Channels

By combining various of contributions from the relevant Feynman diagrams together, the total decay amplitudes for the four penguin-dominated decays $B_{(s)} \rightarrow K_0^* \bar{K}_0^*$ and the pure annihilation processes $B_d \rightarrow K_0^{*+} K_0^{*-}$ and $B_c \rightarrow K_0^{*+} \bar{K}_0^{*0}$ can then read as,

1. The total decay amplitudes of $B \rightarrow K_0^* \bar{K}_0^*$ decays:

$$\begin{aligned} \mathcal{A}(B_u \rightarrow K_0^{*+} \bar{K}_0^{*0}) &= \lambda_u \left[M_{nfa} C_1 \right] - \lambda_t \left[F_{fs} \left(a_4 - \frac{1}{2} a_{10} \right) + F_{fs}^{P2} \left(a_6 - \frac{1}{2} a_8 \right) \right. \\ &\quad \left. + M_{nfs} \left(C_3 - \frac{1}{2} C_9 \right) + M_{nfs} \left(C_5 - \frac{1}{2} C_7 \right) + M_{nfa} \right. \\ &\quad \left. \times \left(C_3 + C_9 \right) + M_{nfa}^{P1} \left(C_5 + C_7 \right) + f_B F_{fa}^{P2} \left(a_6 + a_8 \right) \right], \quad (29) \end{aligned}$$

where $\lambda_u = V_{ub}^* V_{ud}$ and $\lambda_t = V_{tb}^* V_{td}$.

$$\begin{aligned} \mathcal{A}(B_d \rightarrow K_0^{*+} K_0^{*-}) &= \lambda_u \left[M_{nfa} C_2 \right] - \lambda_t \left[M_{nfa} \left(C_4 + C_{10} \right) + M_{nfa}^{P2} \left(C_6 + C_8 \right) \right. \\ &\quad \left. + M_{nfa} \left[K_0^{*+} \leftrightarrow K_0^{*-} \right] \left(C_4 - \frac{1}{2} C_{10} \right) \right. \\ &\quad \left. + M_{nfa}^{P2} \left[K_0^{*+} \leftrightarrow K_0^{*-} \right] \left(C_6 - \frac{1}{2} C_8 \right) \right], \quad (30) \end{aligned}$$

$$\begin{aligned} \mathcal{A}(B_d \rightarrow K_0^{*0} \bar{K}_0^{*0}) &= -\lambda_t \left[F_{fs} \left(a_4 - \frac{1}{2} a_{10} \right) + F_{fs}^{P2} \left(a_6 - \frac{1}{2} a_8 \right) + \left(M_{nfs} + M_{nfa} \right) \right. \\ &\quad \left. \times \left(C_3 - \frac{1}{2} C_9 \right) + \left(M_{nfs}^{P1} + M_{nfa}^{P1} \right) \left(C_5 - \frac{1}{2} C_7 \right) + \left(M_{nfa} \right. \right. \\ &\quad \left. \left. + \left[K_0^{*0} \leftrightarrow \bar{K}_0^{*0} \right] \right) \left(C_4 - \frac{1}{2} C_{10} \right) + \left(M_{nfa}^{P2} + \left[K_0^{*0} \leftrightarrow \bar{K}_0^{*0} \right] \right) \right. \\ &\quad \left. \times \left(C_6 - \frac{1}{2} C_8 \right) + f_B F_{fa}^{P2} \left(a_6 - \frac{1}{2} a_8 \right) \right]; \quad (31) \end{aligned}$$

2. The total decay amplitudes of $B_s \rightarrow K_0^* \bar{K}_0^*$ decays:

$$\begin{aligned} \mathcal{A}(B_s \rightarrow K_0^{*+} K_0^{*-}) &= \lambda'_u \left[F_{fs} a_1 + M_{nfs} C_1 + M_{nfa} C_2 \right] - \lambda'_t \left[F_{fs} \left(a_4 + a_{10} \right) \right. \\ &\quad \left. + F_{fs}^{P2} \left(a_6 + a_8 \right) + M_{nfs} \left(C_3 + C_9 \right) + M_{nfs}^{P1} \left(C_5 + C_7 \right) \right. \\ &\quad \left. + M_{nfa} \left(C_3 - \frac{1}{2} C_9 + C_4 - \frac{1}{2} C_{10} \right) + M_{nfa} \left[K_0^{*+} \leftrightarrow K_0^{*-} \right] \right. \\ &\quad \left. \times \left(C_4 + C_{10} \right) + M_{nfa}^{P1} \left(C_5 - \frac{1}{2} C_7 \right) + M_{nfa}^{P2} \left(C_6 - \frac{1}{2} C_8 \right) \right. \\ &\quad \left. + M_{nfa}^{P2} \left[K_0^{*+} \leftrightarrow K_0^{*-} \right] \left(C_6 + C_8 \right) + f_{B_s} F_{fa}^{P2} \left(a_6 - \frac{1}{2} a_8 \right) \right] \quad (32) \end{aligned}$$

where $\lambda'_u = V_{ub}^* V_{us}$ and $\lambda'_t = V_{tb}^* V_{ts}$.

$$\begin{aligned}
\mathcal{A}(B_s \rightarrow K_0^{*0} \bar{K}_0^{*0}) &= -\lambda'_t \left[F_{fs}(a_4 - \frac{1}{2}a_{10}) + F_{fs}^{P2}(a_6 - \frac{1}{2}a_8) + (M_{nfs} + M_{nfa}) \right. \\
&\quad \times (C_3 - \frac{1}{2}C_9) + (M_{nfs}^{P1} + M_{nfa}^{P1})(C_5 - \frac{1}{2}C_7) + (M_{nfa} \\
&\quad + [K_0^{*0} \leftrightarrow \bar{K}_0^{*0}]) (C_4 - \frac{1}{2}C_{10}) + (M_{nfa}^{P2} + [K_0^{*0} \leftrightarrow \bar{K}_0^{*0}]) \\
&\quad \left. \times (C_6 - \frac{1}{2}C_8) + f_{B_s} F_{fa}^{P2}(a_6 - \frac{1}{2}a_8) \right]; \tag{33}
\end{aligned}$$

3. The total decay amplitude of $B_c \rightarrow K_0^{*+} \bar{K}_0^{*0}$ decay:

$$\mathcal{A}(B_c \rightarrow K_0^{*+} \bar{K}_0^{*0}) = V_{cb}^* V_{ud} \left[f_{B_c} F'_{fa} a_1 + M'_{nfa} C_1 \right]. \tag{34}$$

In the above decay amplitudes for the channels $B_{(s)} \rightarrow K_0^* \bar{K}_0^*$, based on the relevant discussions after Eq. (26), we have neglected the factorizable annihilation contributions F_{fa} in Eqs. (29)-(33) induced from the small SU(3) symmetry breaking effects. However, for the pure annihilation mode $B_c \rightarrow K_0^{*+} \bar{K}_0^{*0}$, to present the large annihilation contribution occurred in this considered B_c decay channel, we therefore have kept the factorizable decay amplitude F'_{fa} in Eq. (34).

IV. NUMERICAL RESULTS AND DISCUSSIONS

In this section, we will make the theoretical predictions on the CP-averaged BRs and CP-violating asymmetries for those considered $B_q \rightarrow K_0^* \bar{K}_0^*$ decay modes. In numerical calculations, central values of the input parameters will be used implicitly unless otherwise stated. Firstly, we shall make several essential discussions on the input quantities.

A. Input Quantities

The pQCD predictions depend on the inputs for the nonperturbative parameters such as decay constants and universal distribution amplitudes for heavy pseudoscalar B_q and light scalar K_0^* mesons. For the B/B_s mesons, the distribution amplitudes in the b space have been proposed

$$\phi_B(x, b) = N_B x^2 (1-x)^2 \exp \left[-\frac{1}{2} \left(\frac{xm_B}{\omega_b} \right)^2 - \frac{\omega_b^2 b^2}{2} \right], \tag{35}$$

in Refs. [21, 22] and

$$\phi_{B_s}(x, b) = N_{B_s} x^2 (1-x)^2 \exp \left[-\frac{1}{2} \left(\frac{xm_{B_s}}{\omega_{b_s}} \right)^2 - \frac{\omega_{b_s}^2 b^2}{2} \right], \tag{36}$$

in Ref. [33], respectively, where the normalization factors $N_{B(s)}$ are related to the decay constants $f_{B(s)}$ through

$$\int_0^1 dx \phi_{B(s)}(x, b=0) = \frac{f_{B(s)}}{2\sqrt{6}}. \quad (37)$$

In recent years, a lot of studies for B decays have been performed in the pQCD approach [21, 22], and the shape parameter ω_b has been fixed at 0.40 GeV by using the rich experimental data on the B mesons with $f_B = 0.19$ GeV. Correspondingly, the normalization constant N_B is 91.745. For B_s meson, considering a small SU(3) symmetry breaking, since s quark is heavier than the u or d quark, the momentum fraction of s quark should be a little larger than that of u or d quark in the B mesons, we therefore adopt the shape parameter $\omega_{bs} = 0.50$ GeV [33] with $f_{B_s} = 0.23$ GeV, then the corresponding normalization constant is $N_{B_s} = 63.67$. In order to analyze the uncertainties of theoretical predictions induced by the inputs, we can vary the shape parameters ω_b and ω_{bs} by 10%, i.e., $\omega_b = 0.40 \pm 0.04$ GeV and $\omega_{bs} = 0.50 \pm 0.05$ GeV, respectively.

As for the double heavy-flavored B_c meson, since it embraces two heavy quarks b and c simultaneously, the distribution amplitude ϕ_{B_c} would be close to $\delta(x - m_c/m_{B_c})$ [36] in the non-relativistic limit, we therefore adopt the non-relativistic approximation form (See [35] and references therein),

$$\phi_{B_c}(x) = \frac{f_{B_c}}{2\sqrt{6}} \delta(x - m_c/m_{B_c}), \quad (38)$$

where f_{B_c} is the decay constant for B_c meson and to be determined by the precision data in principle. Unfortunately, however, there are no available experimental measurements on f_{B_c} , we then adopt the result calculated in Lattice QCD [37],

$$f_{B_c} = (489 \pm 4 \pm 3) \text{ MeV}. \quad (39)$$

For the scalar K_0^* , its leading twist light-cone distribution amplitude $\phi_{K_0^*}(x, \mu)$ can be generally expanded as the Gegenbauer polynomials [10, 38]:

$$\phi_{K_0^*}(x, \mu) = \frac{3}{\sqrt{2N_c}} x(1-x) \left\{ f_{K_0^*}(\mu) + \bar{f}_{K_0^*}(\mu) \sum_{m=1}^{\infty} B_m(\mu) C_m^{3/2}(2x-1) \right\}, \quad (40)$$

where $f_{K_0^*}(\mu)$ and $\bar{f}_{K_0^*}(\mu)$, $B_m(\mu)$, and $C_m^{3/2}(t)$ are the vector and scalar decay constants, Gegenbauer moments, and Gegenbauer polynomials, respectively.

There exists a relation between the vector and scalar decay constants,

$$\bar{f}_{K_0^*} = \mu_{K_0^*} f_{K_0^*} \quad \text{and} \quad \mu_{K_0^*} = \frac{m_{K_0^*}}{m_2(\mu) - m_1(\mu)}, \quad (41)$$

where m_1 and m_2 are the running current quark masses in the scalar K_0^* .

The values for scalar decay constants and Gegenbauer moments in the distribution amplitudes of K_0^* have been investigated at scale $\mu = 1$ GeV in scenarios S1 and S2 [10]:

$$\begin{aligned} \bar{f}_{K_0^*} &= -0.300 \pm 0.030 \text{ GeV}, & B_1 &= 0.58 \pm 0.07, & B_3 &= -1.20 \pm 0.08 & \text{(S1)}, \\ \bar{f}_{K_0^*} &= 0.445 \pm 0.050 \text{ GeV}, & B_1 &= -0.57 \pm 0.13, & B_3 &= -0.42 \pm 0.22 & \text{(S2)}; \end{aligned} \quad (42)$$

As for the twist-3 distribution amplitudes $\phi_{K_0^*}^S$ and $\phi_{K_0^*}^T$, they have been investigated in only S2 with large uncertainties [39]. We therefore adopt the asymptotic forms in our numerical calculations for simplicity:

$$\phi_{K_0^*}^S = \frac{1}{2\sqrt{2N_c}} \bar{f}_{K_0^*}, \quad \phi_{K_0^*}^T = \frac{1}{2\sqrt{2N_c}} \bar{f}_{K_0^*} (1 - 2x). \quad (43)$$

The QCD scale (GeV), masses (GeV), and B_q meson lifetime(ps) are [21, 22, 40]

$$\begin{aligned} \Lambda_{\overline{\text{MS}}}^{(f=4)} &= 0.250, & m_W &= 80.41, & m_{B_c} &= 6.286, & m_{B_s} &= 5.366; \\ m_B &= 5.279, & m_b &= 4.8, & m_c &= 1.5, & m_{K_0^*} &= 1.425; \\ \tau_{B_u} &= 1.638, & \tau_{B_d} &= 1.53, & \tau_{B_s} &= 1.47, & \tau_{B_c} &= 0.46. \end{aligned} \quad (44)$$

For the CKM matrix elements, we adopt the Wolfenstein parametrization and the updated parameters $A = 0.814$, $\lambda = 0.2257$, $\bar{\rho} = 0.135$, and $\bar{\eta} = 0.349$ [40].

Utilizing the above chosen distribution amplitudes and the central values of the relevant input parameters, we can get the numerical results in the pQCD approach for the form factors $F_{0,1}^{B \rightarrow K_0^*}$ and $F_{0,1}^{B_s \rightarrow \bar{K}_0^*}$ from Eq. (15) at maximal recoil as follows,

$$F_{0,1}^{B \rightarrow K_0^*}(q^2 = 0) = \begin{cases} -0.34_{-0.06}^{+0.04}(\omega_b)_{-0.04}^{+0.03}(\bar{f}_S)_{-0.03}^{+0.01}(B_i^S) & \text{(S1)} \\ 0.63_{-0.08}^{+0.10}(\omega_b)_{-0.07}^{+0.07}(f_S)_{-0.06}^{+0.06}(B_i^S) & \text{(S2)} \end{cases}, \quad (45)$$

$$F_{0,1}^{B_s \rightarrow \bar{K}_0^*}(q^2 = 0) = \begin{cases} -0.31_{-0.05}^{+0.05}(\omega_{bs})_{-0.03}^{+0.03}(\bar{f}_S)_{-0.01}^{+0.01}(B_i^S) & \text{(S1)} \\ 0.57_{-0.08}^{+0.09}(\omega_{bs})_{-0.07}^{+0.06}(f_S)_{-0.06}^{+0.05}(B_i^S) & \text{(S2)} \end{cases}. \quad (46)$$

where the errors arise from the shape parameter $\omega_b(\omega_{bs})$ in $B(B_s)$ meson distribution amplitude, the scalar decay constant \bar{f}_S , and the Gegenbauer moments B_i^S in the light K_0^* distribution amplitude, respectively. These values agree well with those as given in Ref. [38].

B. CP-averaged Branching Ratios

In this subsection, we will analyze the CP-averaged BRs of the charmless hadronic $B_q \rightarrow K_0^* \bar{K}_0^*$ decays in the pQCD approach. For $B_q \rightarrow K_0^* \bar{K}_0^*$ decays, the decay rate can be written as

$$\Gamma = \frac{G_F^2 m_{B_q}^3}{32\pi} (1 - 2r_S^2) |\mathcal{A}(B_q \rightarrow K_0^* \bar{K}_0^*)|^2, \quad (47)$$

where the corresponding decay amplitudes \mathcal{A} have been given explicitly in Eqs. (29-34). Using the decay amplitudes obtained in last section, it is straightforward to calculate the CP-averaged BRs with uncertainties as displayed in Eqs. (48)-(50), (51)-(52), and (53). The dominant errors are induced by the uncertainties of the shape parameters $\omega_b = 0.40 \pm 0.04$ GeV for B mesons and $\omega_{bs} = 0.50 \pm 0.05$ GeV for B_s meson, the charm quark mass $m_c = 1.5 \pm 0.15$ GeV for B_c meson, the scalar decay constants \bar{f}_S and the Gegenbauer moments $B_i^S (i = 1, 3)$ for the scalar K_0^* , and CKM matrix elements $(\bar{\rho}, \bar{\eta})$, respectively. It is worth of mentioning that the variation of the CKM parameters has a

little effects on the BRs of these considered $B_q \rightarrow K_0^* \bar{K}_0^*$ decays in the pQCD approach and thus will be neglected in the numerical results as shown in Eqs. (48)-(53).

The pQCD predictions for the CP-averaged BRs of the decays under consideration within errors in both scenarios S1 and S2 are the following,

$$Br(B_u \rightarrow K_0^{*+} \bar{K}_0^{*0}) \approx \begin{cases} 1.1_{-0.2}^{+0.1}(\omega_b)_{-0.4}^{+0.5}(\bar{f}_S)_{-0.2}^{+0.1}(B_i^S) \times 10^{-5} & \text{(S1)} \\ 1.9_{-0.1}^{+0.2}(\omega_b)_{-0.7}^{+1.1}(\bar{f}_S)_{-0.9}^{+1.3}(B_i^S) \times 10^{-5} & \text{(S2)} \end{cases}, \quad (48)$$

$$Br(B_d \rightarrow K_0^{*0} \bar{K}_0^{*0}) \approx \begin{cases} 1.1_{-0.2}^{+0.2}(\omega_b)_{-0.4}^{+0.6}(\bar{f}_S)_{-0.1}^{+0.2}(B_i^S) \times 10^{-5} & \text{(S1)} \\ 2.0_{-0.1}^{+0.0}(\omega_b)_{-0.8}^{+1.0}(\bar{f}_S)_{-1.2}^{+1.7}(B_i^S) \times 10^{-5} & \text{(S2)} \end{cases}, \quad (49)$$

$$Br(B_d \rightarrow K_0^{*+} K_0^{*-}) \approx \begin{cases} 3.2_{-0.1}^{+0.0}(\omega_b)_{-1.1}^{+1.6}(\bar{f}_S)_{-0.8}^{+1.0}(B_i^S) \times 10^{-6} & \text{(S1)} \\ 2.2_{-0.4}^{+0.4}(\omega_b)_{-0.8}^{+1.1}(\bar{f}_S)_{-1.2}^{+1.8}(B_i^S) \times 10^{-6} & \text{(S2)} \end{cases}; \quad (50)$$

$$Br(B_s \rightarrow K_0^{*0} \bar{K}_0^{*0}) \approx \begin{cases} 2.5_{-0.5}^{+0.6}(\omega_{bs})_{-0.9}^{+1.1}(\bar{f}_S)_{-0.4}^{+0.4}(B_i^S) \times 10^{-4} & \text{(S1)} \\ 5.4_{-0.2}^{+0.1}(\omega_{bs})_{-2.1}^{+2.8}(\bar{f}_S)_{-3.3}^{+4.8}(B_i^S) \times 10^{-4} & \text{(S2)} \end{cases}, \quad (51)$$

$$Br(B_s \rightarrow K_0^{*+} K_0^{*-}) \approx \begin{cases} 2.3_{-0.4}^{+0.5}(\omega_{bs})_{-0.8}^{+1.1}(\bar{f}_S)_{-0.4}^{+0.4}(B_i^S) \times 10^{-4} & \text{(S1)} \\ 5.2_{-0.2}^{+0.2}(\omega_{bs})_{-2.0}^{+2.8}(\bar{f}_S)_{-3.1}^{+4.6}(B_i^S) \times 10^{-4} & \text{(S2)} \end{cases}; \quad (52)$$

$$Br(B_c \rightarrow K_0^{*+} \bar{K}_0^{*0}) \approx \begin{cases} 2.1_{-0.6}^{+0.7}(m_c)_{-0.7}^{+1.0}(\bar{f}_S)_{-0.4}^{+0.5}(B_i^S) \times 10^{-4} & \text{(S1)} \\ 3.0_{-0.6}^{+0.7}(m_c)_{-1.1}^{+1.6}(\bar{f}_S)_{-1.8}^{+3.2}(B_i^S) \times 10^{-5} & \text{(S2)} \end{cases}. \quad (53)$$

It is easy to see that above BRs are rather large, in the range of 10^{-6} to 10^{-4} , and can be measured at B factories for the relevant $B_{u,d}$ decays, and at the LHC experiments for the considered B_s/B_c decay modes. More importantly, the pure annihilation decays $B_d \rightarrow K_0^{*+} K_0^{*-}$ and $B_c \rightarrow K_0^{*+} \bar{K}_0^{*0}$ with large BRs can provide important information about the weak annihilation amplitudes and more evidences on the sizable annihilation contributions in B physics, then further shed light on the corresponding annihilation decay mechanism.

By comparison with those of $B/B_s \rightarrow K \bar{K}$ decays [33, 41–44], one can easily find that the pQCD predictions for the BRs of $B/B_s \rightarrow K_0^* \bar{K}_0^*$ channels are much larger than that for the corresponding $B/B_s \rightarrow K \bar{K}$ decays by generally a factor of 10. For the pure annihilation mode $B_d \rightarrow K_0^{*+} K_0^{*-}$, however, the enhancement factor is about 100. The main reason for so large difference is that the QCD behavior for the p -wave scalar K_0^* is very different from that for the s -wave pseudoscalar kaon, which can be seen clearly from their distribution amplitudes [10, 45]: the former governed by the odd Gegenbauer moments, while the latter dominated by the even ones, apart from the small symmetry breaking term a_1^K .

As mentioned in the introduction, up to now, there is only one preliminary upper limit on the branching ratio of $B^0 \rightarrow K_0^{*0} \bar{K}_0^{*0}$ at the 90% confidence level [1–3]:

$$Br(B^0 \rightarrow K_0^{*0} \bar{K}_0^{*0}) < 8.4 \times 10^{-6}, \quad (54)$$

While in the pQCD approach, our theoretical predictions of the BRs for $B^0 \rightarrow K_0^{*0} \bar{K}_0^{*0}$ decay in both scenarios within errors are as follows,

$$Br(B^0 \rightarrow K_0^{*0} \bar{K}_0^{*0}) \approx \begin{cases} 6 \sim 18 \times 10^{-6} & \text{(S1)} \\ 6 \sim 40 \times 10^{-6} & \text{(S2)} \end{cases}, \quad (55)$$

It is easy to see that the pQCD predictions within theoretical errors in both scenarios are consistent with currently available experiment upper limit, and will be tested directly when more data samples are collected at the LHC experiments.

As shown in Eqs. (48)-(53), the pQCD predictions have a strong dependence on the input parameters describing the nonperturbative behavior of the light scalar K_0^* (the scalar decay constant \bar{f}_S and Gegenbauer moments B_i^S), and a moderate dependence on the shape parameters $\omega_b(\omega_{bs})$ in $\phi_B(\phi_{B_s})$ and the charm quark mass m_c in ϕ_{B_c} . Therefore, once the relevant experiments could provide the precise measurements for $B \rightarrow K_0^* \bar{K}_0^*$ modes, one can has a better understanding about the nonperturbative hadron dynamics in K_0^* .

In order to facilitate the discussion, we present the central values of our predictions in terms of the topological amplitudes in Tables I and II, where \mathcal{F}_{fs} , \mathcal{F}_{fa} , \mathcal{M}_{nfs} and \mathcal{M}_{nfa} denote the decay amplitudes from factorizable spectator, factorizable annihilation, nonfactorizable spectator, and nonfactorizable annihilation contributions, respectively.

TABLE I: The factorization decay amplitudes(in unit of 10^{-3} GeV^3) of the charmless hadronic $B_q \rightarrow K_0^* \bar{K}_0^*$ decays in S1, where only the central values are quoted for clarification.

Channels	\mathcal{F}_{fs}	\mathcal{M}_{nfs}	$\mathcal{M}_{nfa}^{(\prime)}$	$\mathcal{F}_{fa}^{(\prime)}$
$B_u \rightarrow K_0^{*+} \bar{K}_0^{*0}$	$1.246 - i0.518$	$0.468 - i0.729$	$-0.733 + i0.335$	$2.540 + i1.614$
$B_d \rightarrow K_0^{*+} K_0^{*-}$	0.0	0.0	$2.070 - i2.517$	$-0.013 + i0.009$
$B_d \rightarrow K_0^{*0} \bar{K}_0^{*0}$	$1.246 - i0.518$	$0.468 - i0.729$	$0.269 - i1.118$	$2.690 + i1.741$
$B_s \rightarrow K_0^{*+} K_0^{*-}$	$-6.020 + i0.190$	$-0.736 + i1.594$	$-2.267 + i5.741$	$-10.190 - i14.192$
$B_s \rightarrow K_0^{*0} \bar{K}_0^{*0}$	-6.270	$-2.732 + i2.310$	$-2.727 + i6.376$	$-10.187 - i14.273$
$B_c \rightarrow K_0^{*+} \bar{K}_0^{*0}$	0.0	0.0	$35.744 - i11.105$	$1.658 - i2.530$

TABLE II: Same as Table I but in S2.

Channels	\mathcal{F}_{fs}	\mathcal{M}_{nfs}	$\mathcal{M}_{nfa}^{(\prime)}$	$\mathcal{F}_{fa}^{(\prime)}$
$B_u \rightarrow K_0^{*+} \bar{K}_0^{*0}$	$2.759 - i1.147$	$-0.364 + i0.377$	$0.601 + i0.407$	$2.528 + i4.018$
$B_d \rightarrow K_0^{*+} K_0^{*-}$	0.0	0.0	$-1.934 + i0.527$	$0.004 - i0.001$
$B_d \rightarrow K_0^{*0} \bar{K}_0^{*0}$	$2.759 - i1.147$	$-0.364 + i0.377$	$-0.800 + i1.260$	$2.629 + i4.035$
$B_s \rightarrow K_0^{*+} K_0^{*-}$	$-13.606 + i0.506$	$0.833 - i1.071$	$4.562 - i4.863$	$-5.022 - i25.089$
$B_s \rightarrow K_0^{*0} \bar{K}_0^{*0}$	-14.158	$2.289 - i0.961$	$4.968 - i4.847$	$-5.293 - i25.192$
$B_c \rightarrow K_0^{*+} \bar{K}_0^{*0}$	0.0	0.0	$-6.626 - i14.063$	$1.387 + i0.083$

Based on the numerical results as shown in Tables I and II, one can easily observe that the factorizable contributions \mathcal{F}_{fs} and \mathcal{F}_{fa} govern the considered four penguin-dominated decay modes $B_u \rightarrow K_0^{*+} \bar{K}_0^{*0}$, $B_d \rightarrow K_0^{*0} \bar{K}_0^{*0}$, $B_s \rightarrow K_0^{*+} K_0^{*-}$, and $B_s \rightarrow K_0^{*0} \bar{K}_0^{*0}$, where

both \mathcal{F}_{f_s} ⁴ and \mathcal{F}_{f_a} are mainly determined by the contributions induced by $(S-P)(S+P)$ operators, e.g., see Eqs. (29) and (31-33); while the nonfactorizable contributions $\mathcal{M}_{nfa}^{(\prime)}$ dominate the rest pure annihilation channel $B_d \rightarrow K_0^{*+}K_0^{*-}$ ($B_c \rightarrow K_0^{*+}\overline{K}_0^{*0}$). The small magnitudes of the factorizable annihilation contributions in $B_d \rightarrow K_0^{*+}K_0^{*-}$ and $B_c \rightarrow K_0^{*+}\overline{K}_0^{*0}$ decays are induced by the tiny SU(3) symmetry breaking effects. The difference between $\mathcal{F}_{f_a}(B_d \rightarrow K_0^{*+}K_0^{*-})$ and $\mathcal{F}'_{f_a}(B_c \rightarrow K_0^{*+}\overline{K}_0^{*0})$ in two scenarios as presented in Tables I and II, however, is mainly governed by two factors apart from $f_{B_c}/f_B \approx 2.6$: one is the ratio of $V_{cb}/V_{ub} \approx 11.5$, the other is the large ratio of $a_1/a_2 \approx 1000$ at the characteristic hard scale $m_b/2$ [33]. The above phenomenological analysis can also be applied to the nonfactorizable annihilation topology. Anyway, one can see that these two considered pure annihilation modes are determined by the contributions arising from the nonfactorizable diagrams, i.e., \mathcal{M}_{nfa} and \mathcal{M}'_{nfa} (See Tables I and II), respectively.

It should be stressed that all these considered $B_q \rightarrow K_0^*\overline{K}_0^*$ decays have large weak annihilation contributions, which can be seen clearly in Tables I and II. It is expected that these decay channels with precision measurements at the experiments will offer a good platform to study the underlying annihilation mechanism.

Using the pQCD predictions, we get the following interesting information on the ratio of the BR's for two sets of considered decays in both scenarios S1 and S2,

$$\frac{\tau_{B_d}}{\tau_{B_u}} \cdot \frac{Br(B_u \rightarrow K_0^{*+}\overline{K}_0^{*0})_{\text{pQCD}}}{Br(B_d \rightarrow K_0^{*0}\overline{K}_0^{*0})_{\text{pQCD}}} \approx 0.9, \quad \frac{Br(B_s \rightarrow K_0^{*0}\overline{K}_0^{*0})_{\text{pQCD}}}{Br(B_s \rightarrow K_0^{*+}K_0^{*-})_{\text{pQCD}}} \approx 1. \quad (56)$$

If these ratios are measured in the near future, they can offer a great opportunity to study the QCD dynamics involved in these four decay channels and will be helpful to test the adopted scenario of the scalar K_0^* in this work.

On the other hand, it is very interesting to notice the ratios among the theoretical BRs of the considered modes in the pQCD approach

$$\frac{Br(B_u \rightarrow K_0^{*+}\overline{K}_0^{*0})_{\text{S2}}}{Br(B_u \rightarrow K_0^{*+}\overline{K}_0^{*0})_{\text{S1}}} \approx \frac{Br(B_d \rightarrow K_0^{*0}\overline{K}_0^{*0})_{\text{S2}}}{Br(B_d \rightarrow K_0^{*0}\overline{K}_0^{*0})_{\text{S1}}} \approx (1.7 \sim 1.8), \quad (57)$$

$$\frac{Br(B_s \rightarrow K_0^{*+}K_0^{*-})_{\text{S2}}}{Br(B_s \rightarrow K_0^{*+}K_0^{*-})_{\text{S1}}} \approx \frac{Br(B_s \rightarrow K_0^{*0}\overline{K}_0^{*0})_{\text{S2}}}{Br(B_s \rightarrow K_0^{*0}\overline{K}_0^{*0})_{\text{S1}}} \approx (2.2 \sim 2.3), \quad (58)$$

$$\frac{Br(B_d \rightarrow K_0^{*+}K_0^{*-})_{\text{S1}}}{Br(B_d \rightarrow K_0^{*+}K_0^{*-})_{\text{S2}}} \approx 1.5, \quad \frac{Br(B_c \rightarrow K_0^{*+}\overline{K}_0^{*0})_{\text{S1}}}{Br(B_c \rightarrow K_0^{*+}\overline{K}_0^{*0})_{\text{S2}}} \approx 7.0. \quad (59)$$

where the central values for the CP-averaged BRs have been quoted. As given in Eqs. (57)-(59), one can easily find that the CP-averaged BRs for the weak annihilation processes

⁴ For the considered decays, $F_{f_s}^{P2}$ with scalar decay constant \bar{f}_S contributes to the magnitude of \mathcal{F}_{f_s} dominantly. This is just because the contributions arising from the vector current operators are very small with the strongly suppressed vector decay constant f_S .

$B_d \rightarrow K_0^{*+} K_0^{*-}$ and $B_c \rightarrow K_0^{*+} \overline{K}_0^{*0}$ in S1 are larger than those in S2 to different extent. While for other four penguin-dominated $B_u \rightarrow K_0^{*+} \overline{K}_0^{*0}$, $B_d \rightarrow K_0^{*0} \overline{K}_0^{*0}$, $B_s \rightarrow K_0^{*0} \overline{K}_0^{*0}$, and $B_s \rightarrow K_0^{*+} K_0^{*-}$ channels, the CP-averaged BRs in the second scenario are larger than those in the first one with a factor around 2. These two different patterns might reveal the different QCD dynamics involved in the corresponding decay channels. The above relevant relations can be confronted with the near future experiments.

C. CP-violating Asymmetries

Now we turn to the evaluations of the CP-violating asymmetries for $B_q \rightarrow K_0^* \overline{K}_0^*$ decays in the pQCD approach.

For the charged B_u and B_c decays, the direct CP-violating asymmetry $\mathcal{A}_{CP}^{\text{dir}}$ can be defined as:

$$\mathcal{A}_{CP}^{\text{dir}} = \frac{|\overline{\mathcal{M}}|^2 - |\mathcal{M}|^2}{|\overline{\mathcal{M}}|^2 + |\mathcal{M}|^2}, \quad (60)$$

where M denotes the decay amplitude of charged $B_{u(c)} \rightarrow K_0^{*+} \overline{K}_0^{*0}$ decays, while \overline{M} stands for the charge conjugation one correspondingly.

Using Eq. (60), it is easy to calculate the direct CP-violating asymmetries as listed in Eq. (61) for the considered B_u decay in S1 and S2,

$$\mathcal{A}_{CP}^{\text{dir}}(B_u \rightarrow K_0^{*+} \overline{K}_0^{*0}) \approx \begin{cases} 33.7_{-2.2}^{+0.2}(\omega_b)_{-0.3}^{+0.6}(\bar{f}_S)_{-3.5}^{+3.5}(B_i^S)_{-1.6}^{+2.0}(\text{CKM})\% & \text{(S1)} \\ -24.4_{-0.3}^{+1.3}(\omega_b)_{-0.4}^{+0.3}(\bar{f}_S)_{-6.9}^{+5.2}(B_i^S)_{-1.6}^{+1.1}(\text{CKM})\% & \text{(S2)} \end{cases}, \quad (61)$$

The large CP-violating asymmetries (61) plus large branching ratios (48) in both scenarios are clearly measurable in the B factories and LHC experiments. If these physical quantities could be tested at the predicted level, it is doubtless that one can determine the better scenario of K_0^* meson and further understand the involved QCD dynamics.

Because only the tree topology is involved, there is no direct CP violation in the considered B_c decay mode, i.e., $\mathcal{A}_{CP}^{\text{dir}}(B_c \rightarrow K_0^{*+} \overline{K}_0^{*0}) = 0$ in both scenarios.

As for the CP-violating asymmetries for the neutral decays $B_{d(s)} \rightarrow K_0^* \overline{K}_0^*$, the effects of $B_{d(s)} - \overline{B}_{d(s)}$ mixing should be considered. The CP-violating asymmetries of $B_{d(s)}(\overline{B}_{d(s)}) \rightarrow K_0^{*+} K_0^{*-}, K_0^{*0} \overline{K}_0^{*0}$ decays are time dependent and can be defined as

$$\begin{aligned} \mathcal{A}_{CP} &\equiv \frac{\Gamma(\overline{B}_{d(s)}(\Delta t) \rightarrow f_{CP}) - \Gamma(B_{d(s)}(\Delta t) \rightarrow f_{CP})}{\Gamma(\overline{B}_{d(s)}(\Delta t) \rightarrow f_{CP}) + \Gamma(B_{d(s)}(\Delta t) \rightarrow f_{CP})} \\ &= \mathcal{A}_{CP}^{\text{dir}} \cos(\Delta m_{(s)} \Delta t) + \mathcal{A}_{CP}^{\text{mix}} \sin(\Delta m_{(s)} \Delta t), \end{aligned} \quad (62)$$

where $\Delta m_{(s)}$ is the mass difference between the two $B_{d(s)}^0$ mass eigenstates, $\Delta t = t_{CP} - t_{tag}$ is the time difference between the tagged $B_{d(s)}^0$ ($\overline{B}_{d(s)}^0$) and the accompanying $\overline{B}_{d(s)}^0$ ($B_{d(s)}^0$) with opposite b flavor decaying to the final CP-eigenstate f_{CP} at the time t_{CP} . The direct and mixing induced CP-violating asymmetries $\mathcal{A}_{CP}^{\text{dir}}(\mathcal{C}_f)$ (or \mathcal{A}_f in term of Belle Collaboration) and $\mathcal{A}_{CP}^{\text{mix}}(\mathcal{S}_f)$ can be written as

$$\mathcal{A}_{CP}^{\text{dir}} = \mathcal{C}_f = \frac{|\lambda_{CP}|^2 - 1}{1 + |\lambda_{CP}|^2}, \quad \mathcal{A}_{CP}^{\text{mix}} = \mathcal{S}_f = \frac{2\text{Im}(\lambda_{CP})}{1 + |\lambda_{CP}|^2}, \quad (63)$$

with the CP-violating parameter λ_{CP}

$$\lambda_{CP} \equiv \eta_f \frac{V_{tb}^* V_{td(s)}}{V_{tb} V_{td(s)}^*} \cdot \frac{\langle f_{CP} | H_{eff} | \overline{B}_{d(s)}^0 \rangle}{\langle f_{CP} | H_{eff} | B_{d(s)}^0 \rangle}. \quad (64)$$

where η_f is the CP-eigenvalue of the final states. Moreover, for B_s meson decays, a non-zero ratio $(\Delta\Gamma/\Gamma)_{B_s}$ is expected in the SM [46, 47]. For $B_s \rightarrow K_0^* \overline{K}_0^*$ decays, the third term $\mathcal{A}_{\Delta\Gamma_s}$ related to the presence of a non-negligible $\Delta\Gamma_s$ to describe the CP violation can be defined as follows [47]:

$$\mathcal{A}_{\Delta\Gamma_s} = \frac{2\text{Re}(\lambda_{CP})}{1 + |\lambda_{CP}|^2}, \quad (65)$$

The three quantities describing the CP violation in B_s meson decays shown in Eqs. (63) and (65) satisfy the following relation,

$$|\mathcal{A}_{CP}^{\text{dir}}|^2 + |\mathcal{A}_{CP}^{\text{mix}}|^2 + |\mathcal{A}_{\Delta\Gamma_s}|^2 = 1. \quad (66)$$

For $B_{(s)}^0/\overline{B}_{(s)}^0 \rightarrow K_0^{*0}\overline{K}_0^{*0}$ decays, they do not exhibit CP violation in both scenarios, since they involve only penguin contributions at the leading order in the SM, as can be seen from the decay amplitudes as given in Eqs. (31) and (33). Then for $B_s^0/\overline{B}_s^0 \rightarrow K_0^{*0}\overline{K}_0^{*0}$ mode, according to Eq. (66), the third term of the CP violation $\mathcal{A}_{\Delta\Gamma_s} = 100\%$. If the experimental data for the direct CP asymmetries $\mathcal{A}_{CP}^{\text{dir}}$ in $B_{d(s)} \rightarrow K_0^{*0}\overline{K}_0^{*0}$ decays exhibit obviously nonzero, which will indicate the existence of new physics beyond the SM and will provide a very promising place to look for this exotic effect.

For $B_{(s)}^0/\overline{B}_{(s)}^0 \rightarrow K_0^{*+}K_0^{*-}$ decays, with the decay amplitudes shown in Eqs. (30) and (32), we can find the numerical results in both scenarios for the CP-violating asymmetries in the pQCD approach are as follows,

$$\mathcal{A}_{CP}^{\text{dir}}(B_d \rightarrow K_0^{*+}K_0^{*-}) \approx \begin{cases} -64.9_{-0.6}^{+0.0}(\omega_b)_{-1.0}^{+0.8}(\overline{f}_S)_{-3.7}^{+5.9}(B_i^S)_{-2.3}^{+4.3}(\text{CKM})\% & \text{(S1)} \\ 5.9_{-0.2}^{+0.3}(\omega_b)_{-2.3}^{+2.7}(\overline{f}_S)_{-1.9}^{+11.2}(B_i^S)_{-0.4}^{+0.2}(\text{CKM})\% & \text{(S2)} \end{cases}, \quad (67)$$

$$\mathcal{A}_{CP}^{\text{mix}}(B_d \rightarrow K_0^{*+}K_0^{*-}) \approx \begin{cases} -49.9_{-6.9}^{+3.8}(\omega_b)_{-0.5}^{+0.4}(\overline{f}_S)_{-4.8}^{+1.7}(B_i^S)_{-8.1}^{+9.0}(\text{CKM})\% & \text{(S1)} \\ -98.9_{-0.2}^{+0.0}(\omega_b)_{-0.1}^{+0.1}(\overline{f}_S)_{-0.9}^{+1.0}(B_i^S)_{-0.6}^{+1.1}(\text{CKM})\% & \text{(S2)} \end{cases}, \quad (68)$$

$$\mathcal{A}_{CP}^{\text{dir}}(B_s \rightarrow K_0^{*+}K_0^{*-}) \approx \begin{cases} 12.9_{-0.1}^{+0.0}(\omega_{bs})_{-0.1}^{+0.1}(\overline{f}_S)_{-1.3}^{+1.6}(B_i^S)_{-0.8}^{+0.6}(\text{CKM})\% & \text{(S1)} \\ -3.2_{-0.4}^{+0.4}(\omega_{bs})_{-0.2}^{+0.3}(\overline{f}_S)_{-1.6}^{+1.5}(B_i^S)_{-0.1}^{+0.2}(\text{CKM})\% & \text{(S2)} \end{cases}, \quad (69)$$

$$\mathcal{A}_{CP}^{\text{mix}}(B_s \rightarrow K_0^{*+}K_0^{*-}) \approx \begin{cases} 3.0_{-1.7}^{+1.6}(\omega_{bs})_{-0.1}^{+0.2}(\overline{f}_S)_{-0.1}^{+0.4}(B_i^S)_{-0.1}^{+0.1}(\text{CKM})\% & \text{(S1)} \\ 1.8_{-0.3}^{+0.2}(\omega_{bs})_{-0.1}^{+0.1}(\overline{f}_S)_{-1.9}^{+0.9}(B_i^S)_{-0.1}^{+0.1}(\text{CKM})\% & \text{(S2)} \end{cases}, \quad (70)$$

$$\mathcal{A}_{\Delta\Gamma_s}(B_s \rightarrow K_0^{*+}K_0^{*-}) \approx \begin{cases} 99.1_{-0.0}^{+0.1}(\omega_{bs})_{-0.0}^{+0.0}(\overline{f}_S)_{-0.2}^{+0.2}(B_i^S)_{-0.1}^{+0.1}(\text{CKM})\% & \text{(S1)} \\ 99.9_{-0.0}^{+0.0}(\omega_{bs})_{-0.0}^{+0.0}(\overline{f}_S)_{-0.0}^{+0.1}(B_i^S)_{-0.0}^{+0.0}(\text{CKM})\% & \text{(S2)} \end{cases}, \quad (71)$$

where the errors are induced by the uncertainties from shape parameter $\omega_b(\omega_{bs})$ for $B(B_s)$ meson, scalar decay constant \bar{f}_S and Gegenbauer moments B_i^S in the distribution amplitudes of scalar K_0^* , and CKM parameters $(\bar{\rho}, \bar{\eta})$, respectively. For the direct CP asymmetries in the $B_d \rightarrow K_0^{*+} K_0^{*-}$ and $B_s \rightarrow K_0^{*+} K_0^{*-}$ decays for example, i.e., Eqs. (67) and (69), one can find that their signs and magnitudes are rather different in both scenarios within theoretical errors. In the former mode, $\mathcal{A}_{CP}^{\text{dir}}$ is $(-69.4 \sim -57.6)$ in S1 and $(2.9 \sim 17.4)$ in S2; while in the latter one, $\mathcal{A}_{CP}^{\text{dir}}$ is $(11.4 \sim 14.6)$ in S1 and $(-4.9 \sim -1.6)$ in S2. But, it is clear to find that the magnitudes of direct CP-violating asymmetries for these two decays in S1 are much larger than those in S2 in the pQCD approach correspondingly, which will be more easily tested by the ongoing LHC and forthcoming SuperB experiments. Furthermore, once the predictions on $\mathcal{A}_{CP}^{\text{dir}}$ including both size and sign in S1 could be confirmed at the predicted level by the stringent experimental measurements in the future, which will be helpful to investigate the physical property of the scalar K_0^* and determine the better scenario describing its QCD dynamics in turn, and vice versa. Meanwhile, the stringent test of $\mathcal{A}_{CP}^{\text{dir}}(B_d \rightarrow K_0^{*+} K_0^{*-})$ can also provide indirect evidences for an important but controversial issue on the evaluation of annihilation contributions at leading power.

Finally, it is worthy of mentioning that we here just study the perturbative short-distance contributions as the first step in present work. The large theoretical errors induced by the large uncertainties of the inputs in the nonperturbative distribution amplitudes, such as ϕ_{B_q} , $\phi_{K_0^*}$, etc, should be constrained by the precision measurements, which will be very helpful to explore the hadronic dynamics of K_0^* and the QCD dynamics involved in these considered decay channels. We do not consider the possible long-distance contributions, such as the rescattering effects, although they should be present, and they may be large and affect the theoretical predictions. It is beyond the scope of this work and expected to be studied in the future.

V. SUMMARY

In this work, we studied the two-body charmless hadronic $B_q \rightarrow K_0^* \bar{K}_0^*(q = u, d, s, c)$ decays by employing the pQCD approach based on the k_T factorization theorem. Based on the assumption of two-quark structure of the light scalar K_0^* , we made the theoretical predictions and phenomenological analysis on the physical observables: CP-averaged branching ratios and CP-violating asymmetries.

From our numerical evaluations and phenomenological analysis, we found the following results:

- In both scenarios of K_0^* , $B_q \rightarrow K_0^* \bar{K}_0^*$ decays in the pQCD approach exhibit the large CP-averaged branching ratios ($10^{-6} \sim 10^{-4}$), which are clearly measurable in the present B factories and ongoing LHC experiments.
- In the considered six decay channels, only preliminary upper limit on $Br(B_d^0 \rightarrow K_0^{*0} \bar{K}_0^{*0})$ mode has been reported. The pQCD prediction basically agrees with this upper limit, and will be tested when better experimental measurements become available.

- For $B_u \rightarrow K_0^{*+} \overline{K}_0^{*0}$ decay, the large branching ratio plus large direct CP-violating asymmetry will offer a great opportunity to test the hadronic dynamics of K_0^* and the QCD dynamics involved in the considered mode.
- The obvious nonzero $\mathcal{A}_{CP}^{\text{dir}}$ for $B_{d(s)} \rightarrow K_0^{*0} \overline{K}_0^{*0}$ decays will provide a good platform to explore the exotic new physics effects beyond the SM.
- The pure annihilation process $B_c \rightarrow K_0^{*+} \overline{K}_0^{*0}$ have a large branching ratio and will be measured soon at the LHC experiments, which can help us to understand the role of the annihilation contributions in B physics.
- The pQCD predictions still have large theoretical uncertainties induced by the uncertainties of input parameters, such as the universal distribution amplitudes ϕ_{B_q} and $\phi_{K_0^*}$, which should be well constrained by the precision data.

Acknowledgments

The authors would like to thank Cai-Dian Lü and Hsiang-Nan Li for helpful discussions. X. Liu thanks Y.M. Wang for his comments. This work is supported by the National Natural Science Foundation of China under Grant No. 10975074, and No. 10735080, and by the Project on Graduate Students' Education and Innovation of Jiangsu Province, under Grant No. CX09B_297Z, and by the Project on Excellent Ph.D Thesis of Nanjing Normal University, under Grant No. 181200000251, and by the Project on Start-up Fund of Xuzhou Normal University.

-
- [1] C.C. Chiang *et al.*, (Belle Collaboration), *Phys. Rev. D* **81**, 071101(R) (2010).
 - [2] K.F. Chen, *Nucl. Phys. B (Proc. Suppl.)* **210-211**, 147 (2011).
 - [3] D. Asner *et al.*, (HFAG), arXiv:1010.1589[hep-ex]; and online update at <http://www.slac.stanford.edu/xorg/hfag>.
 - [4] N. Brambilla *et al.*, (Quarkonium Working Group), CERN-2005-005, arXiv:0412158[hep-ph].
 - [5] N. Mathur *et al.*, *Phys. Rev. D* **76**, 114505 (2007).
 - [6] W. Lee and D. Weingarten, *Phys. Rev. D* **61**, 014015 (1999); M. Göckeler *et al.*, *Phys. Rev. D* **57**, 5562 (1998); S. Kim and S. Ohta, *Nucl. Phys. B (Proc. Suppl.)* **53**, 199 (1997); A. Hart, C. McNeile, and C. Michael, *Nucl. Phys. B (Proc. Suppl.)* **119**, 266 (2003); T. Burch *et al.*, (BGR Collaboration), *Phys. Rev. D* **73**, 094505 (2006).
 - [7] W. Bardeen, A. Duncan, E. Eichten, N. Isgur, and H. Thacker, *Phys. Rev. D* **65**, 014509 (2001).
 - [8] T. Kunihiro *et al.*, (Scalar Collaboration), *Phys. Rev. D* **70**, 034504 (2004).
 - [9] S. Prelovsek, C. Dawson, T. Izubuchi, K. Orginos, and A. Soni, *Phys. Rev. D* **70**, 094503 (2004).
 - [10] H.Y. Cheng, C.K. Chua, and K.C. Yang, *Phys. Rev. D* **73**, 014017 (2006), and reference therein; H.Y. Cheng, C.K. Chua, and K.C. Yang, *Phys. Rev. D* **77**, 014034 (2008).

- [11] M. Beneke, G. Buchalla, and M. Neubert, C.T. Sachrajda, Phys. Rev. Lett. **83**, 1914 (1999); Nucl. Phys. B **591**, 313 (2000); Nucl. Phys. B **606**, 245 (2001).
- [12] D.S. Du, H.J. Gong, J.F. Sun, D.S. Yang, and G.H. Zhu, Phys. Rev. D **65**, 094025 (2002).
- [13] C.H. Chen and C.Q. Geng, Phys. Rev. D **75**, 054010 (2007).
- [14] Y.L. Shen, W. Wang, J. Zhu, and C.D. Lü, Eur. Phys. J. C **50**, 877 (2007).
- [15] C.S. Kim, Y. Li, and W. Wang, Phys. Rev. D **81**, 074014 (2010).
- [16] X. Liu and Z.J. Xiao, Commun. Theor. Phys. **53**, 540 (2010); X. Liu, Z.Q. Zhang, and Z.J. Xiao, Chin. Phys. C **34**, 157 (2010).
- [17] X. Liu and Z.J. Xiao, Phys. Rev. D **82**, 054029 (2010).
- [18] M. Wirbel, B. Stech and M. Bauer, Z. Phys. C **29**, 637 (1985); M. Bauer, B. Stech and M. Wirbel, Z. Phys. C **34**, 103 (1987).
- [19] A. Ali, G. Kramer and C.D. Lü, Phys. Rev. D **58**, 094009 (1998); *ibid.* **59**, 014005 (1999).
- [20] C.W. Bauer, D. Pirjol, and I.Z. Rothstein, I.W. Stewart, Phys. Rev. D **70**, 054015 (2004).
- [21] Y.Y. Keum, H.N. Li, and A.I. Sanda, Phys. Lett. B **504**, 6 (2001); Phys. Rev. D **63**, 054008 (2001).
- [22] C.D. Lü, K. Ukai, and M.Z. Yang, Phys. Rev. D **63**, 074009 (2001).
- [23] H.N. Li, Prog. Part. & Nucl. Phys. **51**, 85 (2003), and reference therein.
- [24] H.N. Li, Proc. Sci, **FPCP2009** (2009) 026.
- [25] J. Chay, H.N. Li, and S. Mishima, Phys. Rev. D **78**, 034037 (2008).
- [26] C.M. Arnesen, Z. Ligeti, and I.Z. Rothstein, I.W. Stewart, Phys. Rev. D **77**, 054006 (2008).
- [27] G. Buchalla, A.J. Buras and M.E. Lautenbacher, Rev. Mod. Phys. **68**, 1125 (1996).
- [28] H.N. Li, Phys. Rev. D **66**, 094010 (2002); H.N. Li and K. Ukai, Phys. Lett. B **555**, 197 (2003).
- [29] J. Botts and G. Sterman, Nucl. Phys. B **325**, 62 (1989).
- [30] H.N. Li and G. Sterman, Nucl. Phys. B **381**, 129 (1992).
- [31] H.N. Li and B. Tseng, Phys. Rev. D **57**, 443 (1998).
- [32] C.D. Lü and M.Z. Yang, Eur. Phys. J. C **28**, 515 (2003).
- [33] A. Ali, G. Kramer, Y. Li, C.D. Lü, Y.L. Shen, W. Wang, and Y.M. Wang, Phys. Rev. D **76**, 074018 (2007);
- [34] X. Liu, H.S. Wang, Z.J. Xiao, L.B. Guo, and C.D. Lü, Phys. Rev. D **73**, 074002 (2006); H.S. Wang, X. Liu, Z.J. Xiao, L.B. Guo, and C.D. Lü, Nucl. Phys. B **738**, 243 (2006); Z.J. Xiao, Z.Q. Zhang, X. Liu, and L.B. Guo, Phys. Rev. D **78**, 114001 (2008).
- [35] X. Liu, Z.J. Xiao, and C.D. Lü, Phys. Rev. D **81**, 014022 (2010); X. Liu and Z.J. Xiao, Phys. Rev. D **81**, 074017 (2010); X. Liu and Z.J. Xiao, J. Phys. G **38**, 035009 (2011).
- [36] G. Bell and Th. Feldmann, J. High Energy Phys. **04**, 061 (2008).
- [37] T.W. Chiu *et al.*, (TWQCD Collaboration), Phys. Lett. B **651**, 171 (2007).
- [38] R.H. Li, C.D. Lü, W. Wang, and X.X. Wang, Phys. Rev. D **79**, 014013 (2009).
- [39] C.D. Lü, Y.M. Wang, and H. Zou, Phys. Rev. D **75**, 056001 (2007).
- [40] C. Amsler *et al.*, (Particle Data Group), Phys. Lett. B **667**, 1 (2008).
- [41] C.H. Chen and H.N. Li, Phys. Rev. D **63**, 014003 (2000).
- [42] M. Beneke and M. Neubert, Nucl. Phys. B **675**, 333 (2003).
- [43] H.Y. Cheng and C.K. Chua, Phys. Rev. D **80**, 11008 (2009).
- [44] H.Y. Cheng and C.K. Chua, Phys. Rev. D **80**, 114026 (2009).
- [45] P. Ball, J. High Energy Phys. **09** (1998) 005; *ibid.* **01** (1999) 010; V.M. Braun and A. Lenz, Phys. Rev. D **70**, 074020 (2004); A. Khodjamirian, Th. Mannel and M. Melcher, Phys.

- Rev. D **70**, 094002 (2004); P. Ball and A. Talbot, J. High Energy Phys. **06** (2005) 063;
P. Ball and R. Zwicky, Phys. Lett. B **633**, 289 (2006).
- [46] M. Beneke, G. Buchalla, C. Greub, A. Lenz and U. Nierste, Phys. Lett. B **459**, 631 (1999).
- [47] L. Fernandez, Ph.D Thesis, CERN-Thesis-2006-042.